Original papers
Materials for energy and environment, next-generation photovoltaics, and green technologies

УДК 661.666 DOI: 10.17277/jamt-2026-11-02-162-171

Synthesis and study of the porous structure of biochars obtained from crustacean waste

© Anastasia E. Memetova[a]✉, Andrey D. Zelenin[a], Viktor S. Yagubov[a], Nariman R. Memetov[a]

[a] *Tambov State Technical University, Bld. 2, 106/5, Sovetskaya St., Tambov, 392000, Russian Federation*

✉ anastasia.90k@mail.ru

Abstract. Biochar samples from crustacean processing waste were synthesized by carbonization followed by alkaline activation. The influence of synthesis parameters (time, temperature) on the porous structure of biochar was considered. The results showed that biomass carbonization conditions significantly affect the final porosity parameters. It was found that the biochar samples obtained by varying the synthesis parameters were micromesoporous. Temperature was shown to be the main influencing factor during biomass carbonization. At a three-hour carbonization duration and a temperature of 650 °C, the specific surface area (2708 $m^2 \cdot g^{-1}$) and pore volume (total pore – 1.58 $cm^3 \cdot g^{-1}$, micropore – 0.64 $cm^3 \cdot g^{-1}$, mesopore – 0.94 $cm^3 \cdot g^{-1}$) in the obtained biochar reached their maximum values. Methane adsorption on the obtained biochar was studied at ambient temperature and pressure up to 100 bar. Biochar obtained from crustacean waste was shown to exhibit a high methane adsorption capacity of ~18 $mmol \cdot g^{-1}$. Experimental adsorption data were analyzed using the Langmuir, Freundlich, and Dubinin-Radushkevich models. The influence of synthesis parameters on the pore structure of biochars, as well as the adsorption data evaluated in the study, are useful for designing adsorption systems.

Keywords: biochar; specific surface area; porosity; biomass carbonization; adsorption.

For citation: Memetova AE, Zelenin AD, Yagubov VS, Memetov NR. Synthesis and study of the porous structure of biochars obtained from crustacean waste. *Journal of Advanced Materials and Technologies*. 2026;11(2):162-171. DOI: 10.17277/jamt-2026-11-02-162-171

Синтез и исследование пористой структуры биоуглей, полученных из отходов ракообразных

© А. Е. Меметова[a]✉, А. Д. Зеленин[a], В. С. Ягубов[a], Н. Р. Меметов[a]

[a] *Тамбовский государственный технический университет, ул. Советская, 106/5, пом. 2, Тамбов, 392000, Российская Федерация*

✉ anastasia.90k@mail.ru

Аннотация. Образцы биоуглей из отходов переработки ракообразных синтезированы путем карбонизации с последующей щелочной активацией. Рассмотрено влияние параметров синтеза (время, температура) на пористую структуру биоугля. Результаты показали, что условия карбонизации биомассы существенно влияют на конечные параметры пористости. Установлено, что образцы биоугля, полученные путем варьирования параметров синтеза, микромезопористые. Показано, что температура является основным влияющим фактором при карбонизации биомассы. При трехчасовой продолжительности карбонизации и температуре 650 °С значения удельной поверхности (2708 $м^2/г$) и объемов пор (общий объем пор – 1,58 $см^3/г$, объем микропор – 0,64 $см^3/г$, объем мезопор – 0,94 $см^3/г$) в полученном биоугле достигали максимального значения. Изучена адсорбция метана на полученном биоугле при температуре окружающей среды и давлении до 100 бар. Показано, что биоуголь из отходов переработки ракообразных демонстрирует высокую адсорбционную способность по метану, равную 18 ммоль/г. Экспериментальные данные адсорбции проанализированы с использованием моделей Ленгмюра, Фрейндлиха и Дубинина-Радушкевича. Влияние параметров синтеза на пористую структуру биоуглей, а также данные адсорбции, оцененные в исследовании, полезны для проектирования адсорбционных систем.

Ключевые слова: биоуголь; площадь удельной поверхности; пористость; карбонизация биомассы; адсорбция.

Для цитирования: Memetova AE, Zelenin AD, Yagubov VS, Memetov NR. Synthesis and study of the porous structure of biochars obtained from crustacean waste. *Journal of Advanced Materials and Technologies*. 2026;11(2):162-171. DOI: 10.17277/jamt-2026-11-02-162-171

1. Introduction

The performance of biochar in various applications is mainly determined by its properties [1, 2]. The surface area and porosity of biochar are among the most important parameters that determine the quantity/quality of available active sites in biochar and, consequently, improve its properties such as cation exchange, water retention, and adsorption capacities [3]. Biochar consists of a wide range of pores, ranging from nanometers to tens of micrometers [4]. The pores can be divided into three groups according to the International Union of Pure and Applied Chemistry (IUPAC) standard: micropores (< 2 nm), mesopores (2–50 nm), and macropores (> 50 nm). In this work, the IUPAC pore standard is used to characterize the pore size distribution. The internal structure of biochar can be estimated from the pore distribution, which is based on the assumption that the complex porous structure in a real solid can be represented by a model with equivalent interactions and regularly shaped pores [5].

Pore size distribution is an important parameter in characterizing the heterogeneity of the biochar porous structure. The surface area is closely related to its porosity. The question of how to obtain biochar with a highly porous structure and large surface area is an active research topic [6].

Over the past ten years, many reviews devoted to biochar have been published. The topics of these reviews mainly focus on the applications of biochar in various fields [7], the relationship between process parameters and biochar characteristics [8], as well as additional modifications for the production of modified biochar [9], and so on. Recent studies have reported the use of shrimp shells to obtain biochars for use as a catalytic support [10], an alternative cathode in fuel cells, supercapacitors [11, 12], an adsorbent of heavy metal ions [13], dyes, and antibiotics [14]. It has also been reported that carbonization parameters have a significant effect on the porosity of the final product [15]. However, biochar obtained by carbonization without subsequent activation has a low specific surface area and porosity [16]. Furthermore, it is important to note that among all activating agents, alkaline activation with KOH is the most effective in producing carbon materials with extremely high specific surface area and pore volume, particularly micropores [17].

At the beginning of the last decade, research on biochar mainly focused on its characteristics in various application areas [18–21]. In the past few years, research has shifted towards studying surface area and porosity [2, 22, 23]. Thus, the efforts of many scientists are aimed at identifying general patterns in the formation of biochar porosity parameters. Various methods and synthesis parameters are used in the production of biochar. It is obvious that the porous structure of biochar changes depending on these parameters. However, the effect of synthesis parameters on the volume and pore size distribution of biochar remains unclear.

In this study, we synthesized biochars from crustacean waste, investigated the influence of synthesis parameters on the development of the porous structure of the resulting materials, and assessed the methane adsorption properties of the biochar with the highest porosity values. As far as we know, the conversion of shrimp waste into highly porous carbon using carbonization followed by KOH activation for methane adsorption has not been previously studied. Therefore, the results of this study offer a promising solution for converting biowaste into a high-tech product for environmental applications.

2. Materials and methods

2.1. Method for producing activated biochar

Shrimp shells were used as the biomass in this study. After removing the meat, the crustacean shells were washed repeatedly with deionized water. The resulting waste was then dried at 110 °C to a constant weight. The crustacean processing waste in the form of a powder with a particle size of < 0.5 mm was loaded into the pilot reactor. The biomass was heated in an argon flow to a predetermined temperature (550–750 °C) and held for various periods of time (2–4 h), and then cooled to room temperature under an argon atmosphere. Next, the resulting carbonizate in the form of a powder with a particle size of < 0.5 mm and granules of 85 % potassium hydroxide with a mass ratio of potassium hydroxide (calculated as 100 % KOH): carbonizate (w/w:2:1) were loaded into the pilot reactor. The reaction mixture was heated to 700°C under an argon flow and held for 2 hours, then cooled to room temperature. After the reactor cooled to room temperature, the reaction mixture was poured with

water, the precipitate was washed to remove alkali until neutral pH, then kept in a hydrochloric acid solution for 24 hours to dissolve metal impurities, after which it was washed again with water and dried at 110 °C to constant weight.

2.2. Analytic methods

To determine the specific surface area, total volume porosity, and micro- and mesoporosity of each sample obtained during the synthesis, an Autosorb-iQ automated adsorption system (Quantachrome, USA) was used. Samples (weighing 1–2 g) prepared for adsorption analysis were degassed at 350 °C for 5 hours under vacuum to remove air, free water, and other impurities before pore structure analysis. At 77 K, N_2 adsorption isotherms were obtained for relative pressures (P/P_0) (gas pressure/vapor pressure) ranging from 0.01 to 0.995. The specific surface area (S_{BET}) was calculated using the Brunauer-Emmett-Teller (BET) equation. The pore size distribution and micropore and mesopore volume were calculated using the Density Functional Theory (DFT) method under the assumption of slit-shaped/cylindrical pores (QSDFT model).

CH_4 adsorption isotherms on the sample at pressures up to 100 bar (at a temperature of 298.15 K) were recorded using an iSorbHP gas adsorption analyzer (Anton Paar GmbH, Graz, Austria). High-purity CH_4 (99.999 % purity; normal boiling point $T_{b.p} = 111.66$ K; critical temperature $T_{cr} = 190.77$ K; critical pressure $P_{cr} = 4.626$ MPa) was used for the measurement. Before the adsorption experiment, the sample was degassed at 350 °C for 5 h.

2.3. Theoretical justification of approaches to determining the specific surface area

Measuring the surface area and porosity of biochar (primarily micro- and mesopores) is typically accomplished using gas adsorption, which involves priming the sample with a given gas atmosphere, recording the adsorption isotherm, and analyzing it accordingly. The most commonly used gas is N_2 (77 K) due to its high availability and low cost.

Both the European Biochar Certificate (EBC) [24] and the International Biochar Initiative (IBI) [25], the most influential biochar organizations worldwide, recommend the BET method for analyzing nitrogen adsorption isotherms to determine surface area [26]. However, the BET method also has some problems. For example, the basic theory of the BET equation is based on a monolayer coating of gas molecules, whereas the primary adsorption mechanism in micropores is pore filling, which inevitably leads to errors in calculating the surface area of biochar. The BET equation is not applicable even for mesopores with widths from 2 to 4 nm due to an overestimation of the monolayer capacity. In the pressure range used in the calculation, not only the formation of monolayer-multilayer structures but also pore filling occurs [27]. Therefore, the BET surface area should be considered as an apparent rather than an absolute surface area, especially for porous materials with a large number of micropores. Despite this, it is still useful for evaluating sorbents for comparative purposes, and the BET surface area is considered a “fingerprint” of the sorbent [28].

For assessing the size distribution, it is advisable to use density functional theory (DFT). This method allows for a more accurate analysis of pore sizes, covering the entire range of mesopores and micropores, unlike other methods, such as the Barrett-Joyner-Halenda (BJH) [29, 30]. In recent years, particular attention has been paid to the DFT method for analyzing pore size distribution. The methane adsorption isotherm was analyzed using the Langmuir, Freundlich, and Dubinin–Radushkevich models [31–33]. An important characteristic of the Langmuir isotherm model is the presence of homogeneous active binding sites on the adsorbent surface, which have identical sorption energies [31]. In contrast, the Freundlich isotherm model assumes a heterogeneous adsorbent surface, namely, different sorption energies. In this case, active binding of adsorbate molecules occurs in areas with higher energy values [33]. The Dubinin–Radushkevich isotherm model is widely used to identify the nature of adsorbate adsorption on an adsorbent and to study the free energy and porosity characteristics of adsorbents [32].

3. Results and Discussion

Traditional technologies for producing highly porous biochars involve carbonization and activation stages, which form a porous structure. Control of the pore structure is possible by varying both the carbonization process conditions (duration, temperature) and the activation process (duration, temperature, and activating agent consumption).

3.1. Effect of carbonization duration on the porous structure of biochars

Process time is a factor that must be considered when conducting the carbonization process. Nitrogen adsorption-desorption isotherms and pore size

distribution curves for biochar samples, obtained at a fixed temperature (t = 550 °C) and variable carbonization time followed by alkaline activation (τ = 2 h; t = 700 °C; w/w: 2/1), are shown in Figs. 1 and 2.

All samples are characterized by similar reversible adsorption isotherms corresponding to combinations of types I and II according to the IUPAC classification (Fig. 1), which is inherent in materials with a wide range of pore size distributions. The hysteresis loops are somewhat similar to adsorption branches corresponding to type H4. This type of loop is often found in micromesoporous carbon materials. In addition to the IUPAC classification, one can refer to the work [34], in which the author identified and correlated five types of hysteresis loops with different pore shapes. Thus, the loop type in the obtained biochar samples (Fig. 1) corresponds to type B, indicating a large number of cylindrical and slit-shaped pores with all sides open.

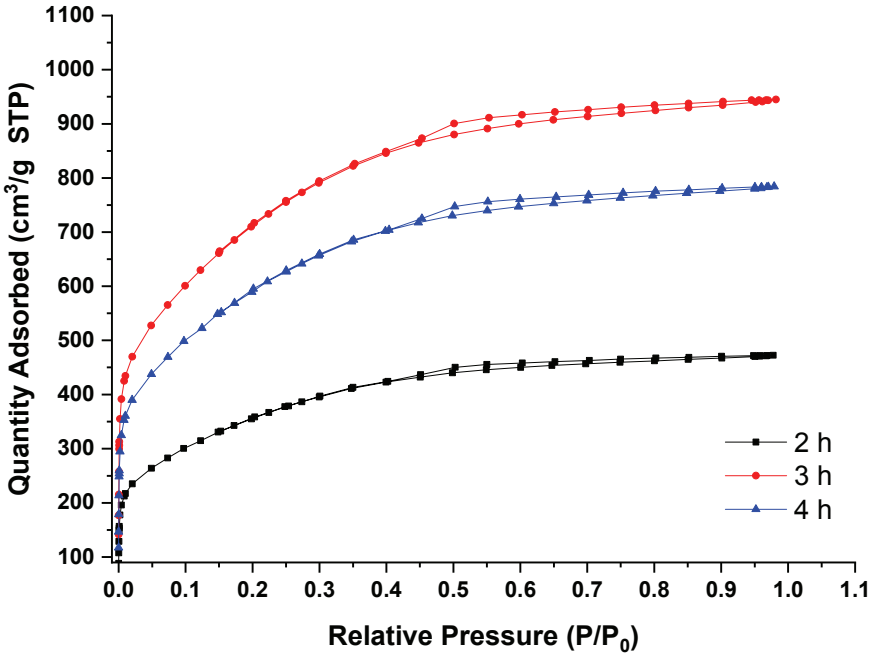

Fig. 1. Nitrogen adsorption-desorption for biochar samples obtained at different carbonization times

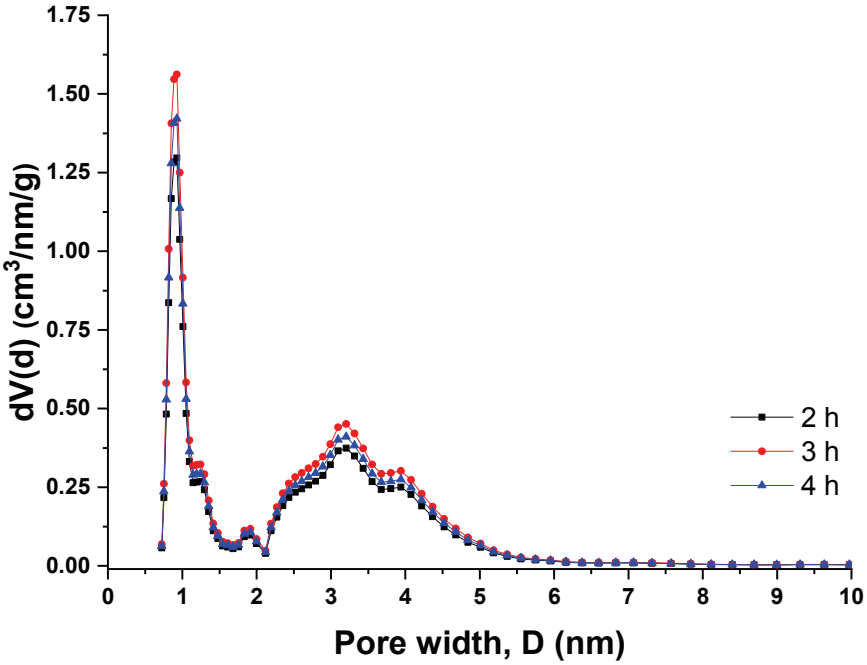

Fig. 2. Pore size distribution for biochar samples obtained at different carbonization times

The pore size distribution curves for the samples (Fig. 2) also exhibit a similar pattern. The results indicate that all of the samples studied exhibit a multimodal pore size distribution. For all samples, the predominant mesopore size ranges from 2 to 6 nm, with a main peak at approximately 3.2 nm. The microporous structure of all of the samples studied appears to be trimodal, with a main peak at 0.92 nm. Thus, the similar appearance of the nitrogen adsorption-desorption isotherm and pore size distributions for the obtained samples indicates that carbonization duration does not significantly influence the porosity type.

In this study, we used the BET and DFT methods to calculate the specific surface area, pore volume, and pore size. The data obtained indicate that sufficient carbonization time results in the complete release of volatiles, which promotes the development of a porous structure. However, excessively long exposure to high temperatures can destroy the pore structure. For example, the biochar surface area increased from 2016 to 2488 $m^2 \cdot g^{-1}$ (BET) and from 1731 to 2120 $m^2 \cdot g^{-1}$ (DFT) with an increase in residence time from 2 to 3 hours, and then decreased to 2121 $m^2 \cdot g^{-1}$ (BET) and 1852 $m^2 \cdot g^{-1}$ (DFT) with an increase in residence time for 4 hours.

Carbonation time also affected the total pore volume (V_p), as well as the micropore (V_{mic}) and mesopore (V_{mes}) volumes of the biochar samples. With increasing carbonation time to 3 h, micro- and mesopore volumes tended to increase, while with a further increase in carbonization duration ($\tau = 4$), they decreased. At a carbonization time of 3 h, the pore volumes in the resulting biochar reached their maximum values ($V_p = 1.37$ $cm^3 \cdot g^{-1}$, $V_{mic} = 0.53$ $cm^3 \cdot g^{-1}$, $V_{mes} = 0.84$ $cm^3 \cdot g^{-1}$).

Thus, the experimental studies demonstrated that carbonization for 3 h promotes the formation of biochars with the best porosity parameters.

3.2. Effect of carbonization temperature on the porous structure of biochars

Carbonization temperature is considered the main parameter influencing the surface area and porosity of biochar. Figures 3 and 4 illustrate this. The nitrogen adsorption-desorption isotherms and pore size distribution curves of biochar samples obtained at different carbonization process temperatures and holding times of 3 h followed by alkaline activation ($\tau = 2$ h; $t = 700$ °C; w/w:2/1) are shown.

All samples exhibit a combination of type I and II isotherms with an H4; B hysteresis loop, which are typical of micromesoporous materials. The maximum amount of nitrogen is adsorbed on the sample obtained at a carbonization temperature of 650 °C. According to the data presented in Fig. 4, micro- and mesopores with diameters less than 6 nm predominate in all samples. The pore structure of all the studied samples, except for the one obtained at 750 °C, is pentamodal, with the main peak at about 0.9 nm. The intensity of the peaks in the range from 0 to 2 nm (insert in Fig. 4) tends to increase.

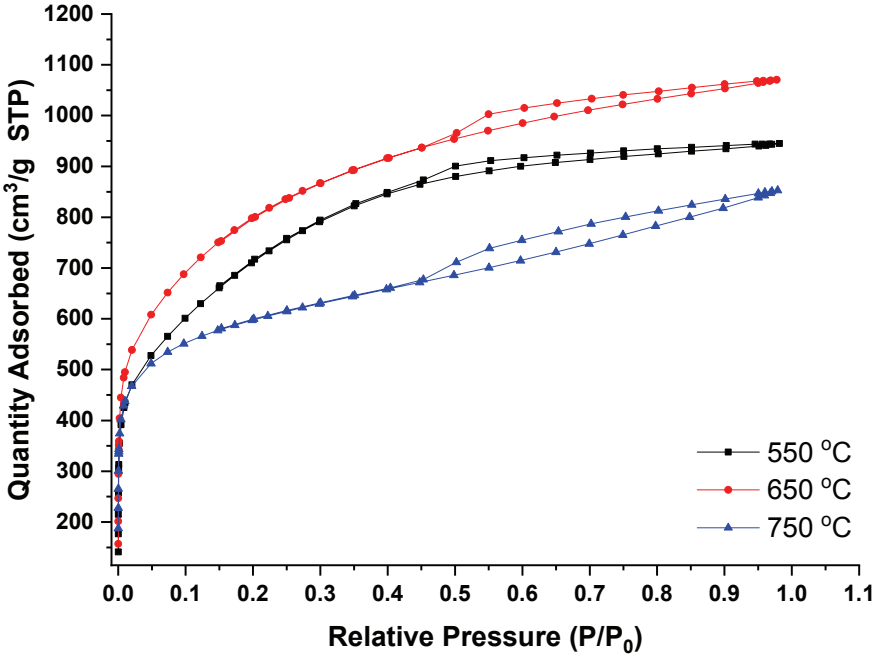

Fig. 3. Nitrogen adsorption-desorption isotherms for biochar samples obtained at different carbonization temperatures

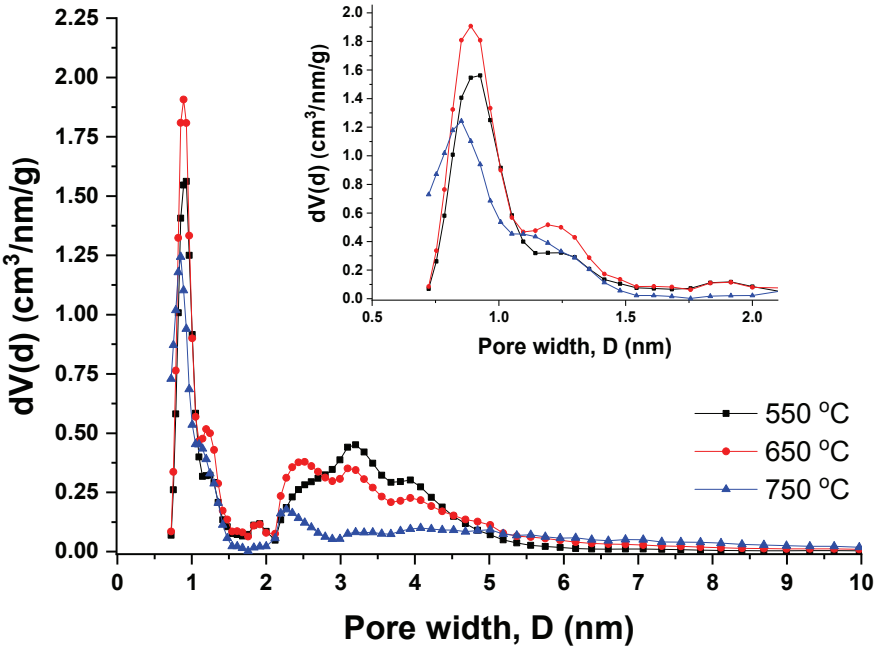

Fig. 4. Pore size distribution for biochar samples obtained at different carbonization temperatures

Table 1. Influence of carbonization temperature on the porosity parameters of biochar samples

Sample	550 °C	650 °C	750 °C
S_{BET}, $m^2 \cdot g^{-1}$	2488	2708	1924
S_{DFT}, $m^2 \cdot g^{-1}$	2102	2384	2158
V_{DFT}, $cm^3 \cdot g^{-1}$	1.37	1.58	1.23
V_{mic}, $cm^3 \cdot g^{-1}$	0.53	0.64	0.64
V_{mes}, $cm^3 \cdot g^{-1}$	0.84	0.94	0.59
V_{01}, $cm^3 \cdot g^{-1}$	0.41	0.46	0.36
V_{02}, $cm^3 \cdot g^{-1}$	0.09	0.17	0.27
V_{03}, $cm^3 \cdot g^{-1}$	0.03	0.27	0.11
V_{04}, $cm^3 \cdot g^{-1}$	0.51	0.23	–
V_{05}, $cm^3 \cdot g^{-1}$	0.33	0.42	0.49
D_{01}, nm	0.92	0.89	0.85
D_{02}, nm	1.24	1.19	1.09
D_{03}, nm	1.91	2.52	2.27
D_{04}, nm	3.20	3.09	–
D_{05}, nm	3.93	3.93	4.82

S_{BET} is the specific surface area for nitrogen calculated by the Brunauer–Emmett–Teller method; S_{DFT} is the specific surface area for nitrogen calculated using the density functional theory; V_{mic} is the specific volume of micropores; V_{mes} is the specific volume of mesopores; V_{01}–V_{05} is the specific volume of pores of the mode; D_{01}–D_{05} is the average diameter (width) of the pores of each mode.

A higher peak intensity value corresponds to a better adsorption capacity of biochar. In other words, on the micropore scale, the sample obtained at a carbonization temperature of 650 °C has the highest adsorption capacity, while the sample obtained at 750 °C has the lowest. These results are in good agreement with the results presented in Table 1.

The sample obtained at 650 °C had the highest specific surface area and pore volumes (S_{BET}= =2708 $m^2 \cdot g^{-1}$, V_p = 1.58 $cm^3 \cdot g^{-1}$, S_{DFT} = 2384 $cm^3 \cdot g^{-1}$, V_{mic} = 0.64 $cm^3 \cdot g^{-1}$, V_{mes}= 0.94 $cm^3 \cdot g^{-1}$).

3.3. Adsorption characteristics of biochar

The adsorption isotherm of excess methane content versus pressure, recorded at ambient temperature (298.15 K), for the biochar sample obtained by carbonization at 650 °C and a holding time of 3 h followed by alkaline activation (τ = 2 h; t = 700 °C; w/w:2/1) is shown in Fig. 5. The presented results show that methane adsorption increases sharply in the initial region (up to approximately 30 bar), then slows down and gradually increases with increasing pressure, showing no tendency to saturate even at 100 bar. The change in the adsorption capacity of the biochar sample as a function of pressure is also shown, approximated by the Langmuir, Freundlich, and Dubinin–Radushkevich models. Results from these models were processed using the equations presented in [31–33].

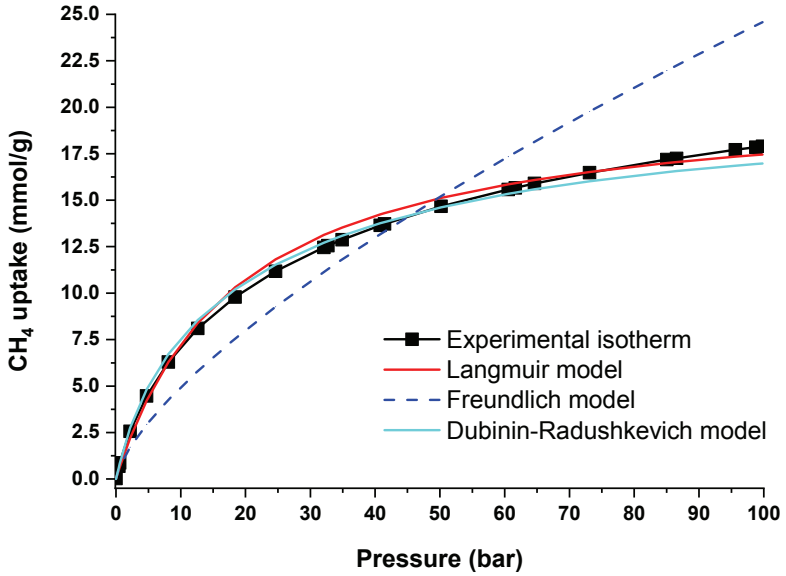

Fig. 5. Adsorption isotherm of CH_4 on a biochar sample obtained at 650 °C adapted to the Langmuir, Freundlich and Dubinin-Radushkevich models

Comparing the data obtained using the models, it can be concluded that they correlate well with the Langmuir ($R^2 = 0.9939$) and Dubinin–Radushkevich ($R^2 = 0.9975$) equations and best describe the process of methane adsorption on the biochar sample in the pressure range considered in this study. However, evaluating the reliability of the models used by the normalized standard deviation (Δa), defined as [35], it can be concluded that the Dubinin–Radushkevich equation (Δa = less than 5 %) describes the studied adsorption process on biochar more accurately than the Langmuir equation (Δa = less than 10 %). The results of processing the experimental data using the Langmuir, Freundlich, and Dubinin–Radushkevich models are presented in Table 2.

The deviation of the limiting methane sorption capacity for the Langmuir (a_L), and Dubinin–Radushkevich ($a_{D–R}$) models from the experimentally obtained value (a_{ekp}) did not exceed ~2 and ~5 %, respectively. The limiting values of micropore adsorption capacity (a_0), calculated using the Dubinin-Radushkevich equation, deviate from a_{ekp} by no more than 2%.

Table 2. Adsorption isotherm coefficients for the Langmuir, Freundlich and Dubinin–Radushkevich models

a_{ekp}, mmol·g^{-1}	Langmuir model constants				
	a_L, mmol·g^{-1}	A, mmol·g^{-1}	b	R^2	Δa, %
	17.5	20.7	0.0539	0.9939	9.93
	Freundlich model constants				
17.9	a_F, mmol·g^{-1}	k	$1/n$	R^2	Δa, %
	24.6	0.9915	0.6974	0.9654	31.02
	Constants of the Dubinin-Radushkevich model				
	$a_{D–R}$	a_0	E	R^2	Δa, %
	17.0	18.2	22.91	0.9975	4.61

S_{BET} – a_L, a_F, $a_{D–R}$ are theoretical values of equilibrium gas adsorption according to the Langmuir, Freundlich and Dubinin–Radushkevich models, respectively, mmol·g^{-1}; A and a_0 are the limiting values of gas adsorption according to the Langmuir and Dubinin–Radushkevich models, respectively, mmol·g^{-1}; b and k are the equilibrium constants according to the Langmuir–Freundlich models, respectively; n is an empirical parameter that characterizes the interaction energy in the adsorbent-adsorbate system; E is the characteristic adsorption energy of the gas under study, kJ·mol^{-1}.

The Dubinin–Radushkevich equation was used to establish the nature of the methane adsorption process on biochar. Based on the obtained values of the characteristic adsorption energy (E = ~23 kJ·mol^{-1}), it is clear that the mechanism is physical in nature [36].

4. Conclusion

Biochar samples were obtained from crustacean processing waste. The influence of carbonization parameters on the development of the porous structure of the biochars was studied. Carbonization temperature can modulate the pore structure of biochars. A three-hour biomass carbonization process at 650°C proved to be most favorable for the development of high specific surface area and pore volumes (S_{BET}= 2708 m^2·g^{-1}, V_p = 1.58 cm^3·g^{-1}, V_{mic} = 0.64 cm^3·g^{-1}, V_{mes}= 0.94 cm^3·g^{-1}). This sample is a micromesoporous material exhibiting high methane adsorption capacity, amounting to 18 mmol·g^{-1} at room temperature and 100 bar.

Thus, this study demonstrates that crustacean waste carbon material is a highly porous and promising biosorbent for methane adsorption.

5. Funding

This study was supported by grant No. 26-16-20053 from the Russian Science Foundation.

Финансирование

Исследование выполнено за счет средств гранта Российского научного фонда № 26-16-20053.

6. Conflict of interests

The authors declare no conflict of interest.

Конфликт интересов

Авторы заявляют об отсутствии конфликта интересов.

References

1. Mohanty AK, Vivekanandhan S, Das O, et al. Biocarbon materials. *Nature Reviews Methods Primers.* 2024;4(1):19. DOI:10.1038/s43586-024-00297-4

2. Zhang Z, Lei Y, Li D, et al. Sudden heating of H3PO4-loaded coconut shell in CO_2 flow to produce super activated carbon and its application for benzene adsorption. *Renewable Energy.* 2020;153:1091-1099. DOI:10.1016/j.renene.2020.02.059

3. Weber K, Quicker P. Properties of biochar. *Fuel.* 2018;217:240-261. DOI:10.1016/j.fuel.2017.12.054

4. Sing KSW. Reporting physisorption data for gas/solid systems with special reference to the determination of surface area and porosity (Recommendations 1984). *Pure and Applied Chemistr.* 1985;57(4):603-619. DOI:10.1351/pac198557040603

5. Hu S, Xiang J, Sun L, Xu M, Qiu J, Fu P. Characterization of char from rapid pyrolysis of rice husk. *Fuel Processing Technology*. 2008;89(11):1096-1105. DOI:10.1016/j.fuproc.2008.05.001

6. Memetova A, Tyagi I, Karri RR, et al. Synthesis of carbon energized materials with directed regulation of specific surface and pore structure as potential adsorbent for methane mitigation. *Journal of Environmental Chemical Engineering.* 2022;10(6):108929. DOI:10.1016/j.jece.2022.108929

7. Wan Z, Sun Y, Tsang DCW, et al. Customised fabrication of nitrogen-doped biochar for environmental and energy applications. *Chemical Engineering Journal.* 2020;401:126136. DOI:10.1016/j.cej.2020.126136

8. Panwar NL, Pawar A. Influence of activation conditions on the physicochemical properties of activated biochar: a review. *Biomass Conversion and Biorefiner.* 2022;12(3):925-947. DOI:10.1007/s13399-020-00870-3

9. Wan Z, Sun Y, Tsang DCW, et al. Sustainable remediation with an electroactive biochar system: mechanisms and perspectives. *Green Chemistry.* 2020;22(9):2688-2711. DOI:10.1039/D0GC00717J

10. Ni J, Li Q, Gong L, et al. Highly efficient chemoenzymatic cascade catalysis of biomass into furfurylamine by a heterogeneous shrimp shell-based chemocatalyst and an ω-transaminase biocatalyst in deep eutectic solvent-water. *ACS Sustainable Chemistry & Engineering*. 2021;9(38):13084-13095. DOI:10.1021/acssuschemeng.1c05109

11. Zhang H, Sun Q, He Q, et al. Single Cu atom dispersed on S,N-codoped nanocarbon derived from shrimp shells for highly-efficient oxygen reduction reaction. *Nano Research.* 2022;15(7):5995-6000. DOI:10.1007/s12274-022-4289-3

12. Zheng FY, Li R, Ge S, Xu WR, Zhang Y. Nitrogen and phosphorus co-doped carbon networks derived from shrimp shells as an efficient oxygen reduction catalyst for microbial fuel cells. *Journal of Power Sources.* 2020;446:227356. DOI:10.1016/j.jpowsour.2019.227356

13. Abomosallam M, Elalfy M, Zheng Z, Nagata K, Suzuki M. Adsorption kinetics and thermodynamics of toxic metal ions onto chitosan nanoparticles extracted from shrimp shells. *Nanotechnology for Environmental Engineering.* 2022;7(1):35-47. DOI:10.1007/s41204-021-00179-0

14. Chen S, Cai H, Du X, et al. Adsorption behavior of hierarchical porous biochar from shrimp shell for tris(2-chloroethyl) phosphate (TCEP): Sorption experiments and DFT calculations. *Environmental Research.* 2023;219:115128. DOI:10.1016/j.envres.2022.115128

15. Yu J, Tang L, Pang Y, et al. Hierarchical porous biochar from shrimp shell for persulfate activation: A two-electron transfer path and key impact factors. *Applied*

Catalysis B: Environmental. 2020;260:118160. DOI: 10.1016/j.apcatb.2019.118160

16. Oginni O, Singh K, Oporto G, Dawson-Andoh B, McDonald L, Sabolsky E. Effect of one-step and two-step H_3PO_4 activation on activated carbon characteristics. *Bioresource Technology Reports.* 2019;8:100307. DOI: 10.1016/j.biteb.2019.100307

17. Ludwinowicz J, Jaroniec M. Effect of activating agents on the development of microporosity in polymeric-based carbon for CO_2 adsorption. *Carbon.* 2015;94:673-679. DOI:10.1016/j.carbon.2015.07.052

18. Yang F, Wang J, Liu L, et al. Synthesis of porous carbons with high N-content from shrimp shells for efficient CO_2 – capture and gas separation. *ACS Sustainable Chemistry & Engineering.* 2018;6(11):15550-15559. DOI:10.1021/acssuschemeng.8b03995

19. Yuan X, Wang J, Deng S, et al. Sustainable food waste management: synthesizing engineered biochar for CO_2 capture. *ACS Sustainable Chemistry & Engineering.* 2022;10(39):13026-13036. DOI:10.1021/acssuschemeng.2c03029

20. Shao S, Wang Y, Ma L, Huang Z, Li X. Sustainable preparation of hierarchical porous carbon from discarded shells of crustaceans for efficient CO_2 capture. *Fuel.* 2024;355:129287. DOI:10.1016/j.fuel.2023.129287

21. Liu C, Huang L, Wei S, et al. Valorized shrimp shell-derived aerogel for trace enrofloxacin removal from aquaculture wastewater: adsorption performance and mechanisms exploration. *Gels.* 2026;12(3):247. DOI:10.3390/gels12030247

22. Zhang Y, Song X, Xu Y, Shen H, Kong X, Xu H. Utilization of wheat bran for producing activated carbon with high specific surface area via NaOH activation using industrial furnace. *Journal of Cleaner Production.* 2019;210:366-375. DOI:10.1016/j.jclepro.2018.11.041

23. Zhang Y, Song X, Zhang P, Gao H, Ou C, Kong X. Production of activated carbons from four wastes via one-step activation and their applications in Pb^{2+} adsorption: Insight of ash content. *Chemosphere.* 2020; 245:125587. DOI:10.1016/j.chemosphere.2019.125587

24. Schmidt HP. *European biochar certificate (EBC) – guidelines version 6.1.* Preprint posted online 2015. DOI:10.13140/RG.2.1.4658.7043

25. Gerlach FM, Szecsenyi J. Family doctor-centred care in Baden-Wuerttemberg: concept and results of a controlled evaluation study. *Zeitschrift für Evidenz, Fortbildung und Qualität im Gesundheitswesen.* 2013;107(6):365-371. DOI:10.1016/j.zefq.2013.07.002

26. Brunauer S, Emmett PH, Teller E. Adsorption of gases in multimolecular layers. *Journal of the American Chemical Society.* 1938;60(2):309-319. DOI:10.1021/ja01269a023

27. Cychosz KA, Guillet-Nicolas R, García-Martínez J, Thommes M. Recent advances in the textural characterization of hierarchically structured nanoporous materials. *Chemical Society Reviews.* 2017;46(2):389-414. DOI:10.1039/C6CS00391E

28. Sdanghi G, Canevesi RLS, Celzard A, Thommes M, Fierro V. Characterization of carbon materials for hydrogen storage and compression. *C.* 2020;6(3):46. DOI:10.3390/c6030046

29. Tarazona P. Free-energy density functional for hard spheres. *Physical Review A.* 1985;31(4):2672-2679. DOI:10.1103/PhysRevA.31.2672

30. Tarazona P, Evans R. A simple density functional theory for inhomogeneous liquids: Wetting by gas at a solid-liquid interface. *Molecular Physics.* 1984;52(4):847-857. DOI:10.1080/00268978400101601

31. Langmuir I. The adsorption of gases on plane surfaces of glass, mica and platinum. *Journal of the American Chemical Society.* 1918;40(9):1361-1403. DOI:10.1021/ja02242a004

32. Dubinin MM. Generalization of the theory of volume filling of micropores to nonhomogeneous microporous structures. *Carbon.* 1985;23(4):373-380. DOI:10.1016/0008-6223(85)90029-6

33. Hu W, Duan S, Chen Y, Zhang Y, Xie Y, Li G. Adsorption characteristics of methane on microporous carbon prepared from bitumite: Equilibrium, thermodynamics and site energy distribution studies. *Journal of Industrial and Engineering Chemistry.* 2025;148:701-723. DOI:10.1016/j.jiec.2025.01.028

34. De Boer JH. The structure and properties of porous materials. In: *Proceedings of the Tenth Symposium of the Colston Research Society Held in the University of Bristol*. London: Butterworths Scientific Publications; 1958. p. 68-94.

35. Tan IAW, Ahmad AL, Hameed BH. Adsorption isotherms, kinetics, thermodynamics and desorption studies of 2,4,6-trichlorophenol on oil palm empty fruit bunch-based activated carbon. *Journal of Hazardous Materials.* 2009;164(2-3):473-482. DOI:10.1016/j.jhazmat.2008.08.025

36. Chen S, Qin C, Wang T, et al. Study on the adsorption of dyestuffs with different properties by sludge-rice husk biochar: Adsorption capacity, isotherm, kinetic, thermodynamics and mechanism. *Journal of Molecular Liquids.* 2019;285:62-74. DOI:10.1016/j.molliq.2019.04.035

Information about the authors / Информация об авторах

Anastasia E. Memetova, Cand. Sc. (Eng.), Associate Professor, Tambov State Technical University (TSTU), Tambov, Russian Federation; ORCID 0000-0002-1036-7389; e-mail: Anastasia.90k@mail.ru

Меметова Анастасия Евгеньевна, кандидат технических наук, доцент, Тамбовский государственный технический университет (ТГТУ), Тамбов, Российская Федерация; ORCID 0000-0002-1036-7389; e-mail: Anastasia.90k@mail.ru

Andrey D. Zelenin, Cand. Sc. (Eng.), Junior Research, TSTU, Tambov, Russian Federation; ORCID 0000-0002-2399-9510; e-mail: zeleandrey@yandex.ru

Viktor S. Yagubov, Cand. Sc. (Eng.), Senior Researcher, TSTU, Tambov, Russian Federation; ORCID 0000-0003-4855-0530; e-mail: vitya-y@mail.ru

Nariman R. Memetov, Cand. Sc. (Eng.), Associate Professor, Head of the Department, TSTU, Tambov, Russian Federation; ORCID 0000-0002-7449-5208; e-mail: mnr979@gmail.com

Зеленин Андрей Дмитриевич, кандидат технических наук, младший научный сотрудник, ТГТУ, Тамбов, Российская Федерация; ORCID 0000-0002-2399-9510; e-mail: zeleandrey@yandex.ru

Ягубов Виктор Сахибович, кандидат технических наук, старший научный сотрудник, ТГТУ, Тамбов, Российская Федерация; ORCID 0000-0003-4855-0530; e-mail: vitya-y@mail.ru

Меметов Нариман Рустемович, кандидат технических наук, доцент, заведующий кафедрой, ТГТУ, Тамбов, Российская Федерация; ORCID 0000-0002-7449-5208; e-mail: mnr979@gmail.com

Received 15 May 2026; Revised 19 June 2026; Accepted 22 June 2026